

A Full Wave Simulation on the Density Dependence of a Slow Wave Excitation in the GAMMA 10/PDX Central Cell with TASK/WF3D^{*)}

Ryuya IKEZOE, Yushi KUBOTA¹⁾, Makoto ICHIMURA¹⁾, Mafumi HIRATA¹⁾, Shuhei SUMIDA¹⁾, Seowon JANG¹⁾, Koki IZUMI¹⁾, Atsuto TANAKA¹⁾, Ryo SEKINE¹⁾, Hiroki KAYANO¹⁾, Yoriko SHIMA¹⁾, Junko KOHAGURA¹⁾, Masayuki YOSHIKAWA¹⁾, Mizuki SAKAMOTO¹⁾, Yousuke NAKASHIMA¹⁾ and Atsushi FUKUYAMA²⁾

Research Institute for Applied Mechanics, Kyushu University, Kasuga 816-8580, Japan

¹⁾*Plasma Research Center, University of Tsukuba, Tsukuba 305-8577, Japan*

²⁾*Department of Nuclear Engineering, Kyoto University, Kyoto 615-8540, Japan*

(Received 30 September 2018 / Accepted 15 November 2018)

Beach heating using a slow Alfvén wave in ion cyclotron range of frequencies would be the first candidate for ion heating in a DEMO-relevant divertor testing linear plasma device if it is applicable to a high-density regime. To clarify its availability, the density dependence of a slow wave excitation is investigated using a full wave simulation with TASK/WF3D code in the GAMMA 10/PDX central cell configuration, where there is an extensive track record of a beach heating. A shielding effect is successfully demonstrated and well understood under a three-dimensional configuration in the limit of cold plasma approximation. As the density increases, excitable left-handed electric field, which contributes to ion cyclotron heating, degrades more and more from a core region, and resultantly the ion absorption region goes outwards with reducing its power. For core densities above 10^{20} m^{-3} , the wave field exists only at a very edge, and ion heating becomes negligible unless the wave frequency is much increased with a correspondent magnetic field enhancement.

© 2019 The Japan Society of Plasma Science and Nuclear Fusion Research

Keywords: slow wave, wave excitation, shielding effect, full wave calculation, mirror plasma

DOI: 10.1585/pfr.14.2402003

1. Introduction

Handling of huge particle and heat fluxes to plasma-facing components and PWI raises concerns to the availability of a fusion reactor. Long time scales and high cycle numbers expected in DEMO put a huge step [1, 2]. However, current confinement experiments do not cover the operational conditions expected in a future fusion reactor. Thus, in order to meet the testing requirements, various kinds of linear plasma devices have been developed and in use [3, 4]. While the required conditions have been partly attained on several devices, no device can offer all the requirements at the same time. To develop a conceptual design for an ultimate linear device which meets a real DEMO-compatible environment, one of the most difficult tasks would be the achievement of ion temperature of about 100 eV with a significant density of over 10^{20} m^{-3} . Existing steady-state high-density linear plasma devices use a plasma source such as a DC arc discharge, an ECR discharge and a helicon plasma, all of which use a high-pressure fuel gas and do not have an active ion heating mechanism. Therefore, increase of ion temperature is

of great difficulty.

Ion cyclotron range of frequencies (ICRF) heating using a slow Alfvén wave excited from a high-field side, which is called as beach heating, would be the first candidate if it is applicable to a high-density linear plasma because a beach heating provides an efficient ion heating and is essentially appropriate for a steady operation. In the GAMMA 10/PDX tandem mirror, hydrogen plasma is produced and heated solely by ICRF waves [5, 6]. The ion temperature is several keV in the perpendicular direction to a magnetic field line and 100–400 eV in the parallel direction for standard operations, where a 6.36 MHz slow wave is used under a magnetic field strength of about 0.4 T and electron density of about $2 \times 10^{18} \text{ m}^{-3}$. Recently, a beach heating of a deuterium helicon plasma with a relatively high density of a few 10^{19} m^{-3} has been tried in proto-MPEX [7], and the increase of ion temperature was observed although it occurred only at the plasma periphery [8].

In order to assess the applicability of a beach heating using a slow wave for ion heating of a future high-density linear plasma device, we have been promoting three studies in GAMMA 10/PDX; they are (i) production of a high-

author's e-mail: ikezo@triam.kyushu-u.ac.jp

^{*)} This article is based on the presentation at the 12th International Conference on Open Magnetic Systems for Plasma Confinement (OS2018).

density target plasma in GAMMA 10/PDX and ion heating experiments in a higher density regime, (ii) development of wave measurements and (iii) evaluation of wave excitation with a help of simulations. As for (i), production and sustainment of a double the typical electron density, of about $4 \times 10^{18} \text{ m}^{-3}$, was achieved by a phase-control ICRF heating [9, 10]. Furthermore, an ECR plasma with the density of about $1 \times 10^{19} \text{ m}^{-3}$ was produced by using a 28 GHz gyrotron although it was still transient, and thus, found to be difficult for ion heating experiments at present. As for (ii), a two-channel microwave reflectometer for wave studies was developed, which provides an antenna switching for a multipoint detection in the axial direction and a simultaneous two-point measurement for wavenumber detection [11, 12]. This paper corresponds to (iii), describing the first investigation on the density dependence of a slow wave excitation in the GAMMA 10/PDX central cell configuration based on a full wave calculation using TASK/WF3D code, which is developed in Kyoto University by one of the authors (A. Fukuyama) [13].

2. Simulation Setting for TASK/WF3D Code

TASK/WF3D is a three-dimensional full wave code solving Maxwell's equation as a boundary-value problem with three-dimensional finite element method. It has been successfully applied to the GAMMA 10/PDX configuration along with its two-dimensional version TASK/WF [14, 15]. Basic equations are shown in such as [15]. Absorption power is treated by adopting a collisional cold plasma model, where the effect of collisions is included in the dielectric tensor. The absorption occurs near a cyclotron resonance layer by the collisional effects.

The calculation conditions such as a magnetic field configuration and ICRF antenna configuration, are set to those of the GAMMA 10/PDX central cell. The magnetic field strength is about 0.4 T and 2.0 T at the midplane and the throat, respectively, consisting of an axisymmetric mirror field. The plasma diameter and the axial length between the mirror throats are 0.36 m and 5.60 m, respectively. The grids are separated by 1.5 cm and 2.0 cm in the axial direction for $|z| < 1.5 \text{ m}$ and $1.5 \text{ m} < |z| < 3.0 \text{ m}$, respectively, where z axis is in the direction of the magnetic field line at the plasma center with the origin at the midplane. In the radial direction, the grids are separated by 2.2 cm and 7.0 cm for $r_{cc} < 27.0 \text{ cm}$ and $27.0 < r_{cc} < 34.0 \text{ cm}$, respectively, where r_{cc} is the radius at the midplane and varies along a magnetic field line.

The shape of the density profile used in this study is determined based on the typical GAMMA 10/PDX discharges and is fixed with varying a peak density from about $1 \times 10^{17} \text{ m}^{-3}$ to $1 \times 10^{21} \text{ m}^{-3}$. As an example, the density profile for $1 \times 10^{18} \text{ m}^{-3}$ is shown in Fig. 1 along with the magnetic field configuration. A tenuous plasma is located outside of the confined plasma. The density of the tenuous

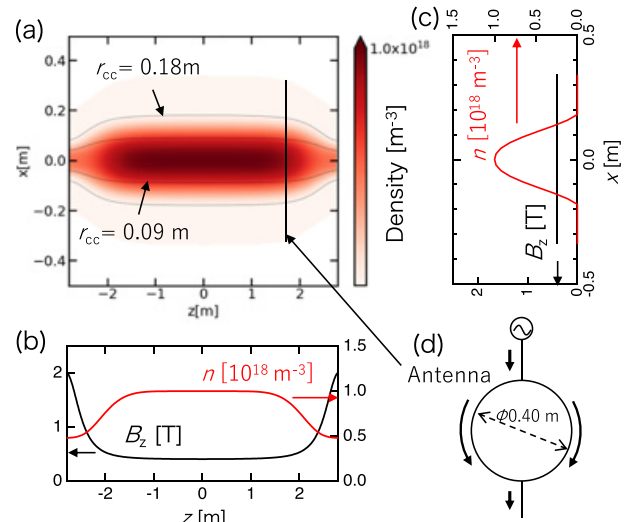


Fig. 1 Electron density profile with a peak density of $1 \times 10^{18} \text{ m}^{-3}$ (a) in x and z plane, and its cross sections at (b) $x = 0$, (c) $z = 0$ along with the magnetic field profile, and (d) a schematic of the double-half-turn RF line current simulating the ICRF antenna.

plasma is uniform and is set to $1 \times 10^{15} \text{ m}^{-3}$ for all the density profiles used in this study. It is confirmed that its value does not affect much the wave structure inside the plasma. At the outside of both mirror throat, a high-density plasma is introduced to simulate a propagation boundary preventing a reflection by increasing a collision frequency.

To closely see a density dependence of wave excitation, single antenna is fed and the other antennas are not in use in this study. The configuration of all the ICRF antennas is shown in such as [9]. The double-half-turn (DHT) antenna in the west side of the central cell is simulated by a DHT line RF current at $z = 171.5 \text{ cm}$ with diameter of 20.0 cm. The frequency of an induced RF current is 6.36 MHz and the amplitude is 620 A. It is confirmed that the excited wave intensity is proportional to the antenna current in this calculation; no nonlinear plasma reaction is included.

3. Full Wave Simulation on the Density Dependence of a Slow Wave Excitation

Figure 2 shows the spatial distribution of calculated ion absorption power for four different densities. The dotted curves show the magnetic field lines at the edge and the half plasma radius. For the peak density of $3 \times 10^{18} \text{ m}^{-3}$, a significant absorption occurs near the ion cyclotron resonance layer in a core region while as the density increases, the absorption region goes outwards in the radial direction with weakening its power. In the middle of 10^{19} m^{-3} , absorption occurs only at a periphery. For $1 \times 10^{20} \text{ m}^{-3}$, ion absorption inside the plasma is greatly reduced and so it does not contribute much to ion heating of the plasma of

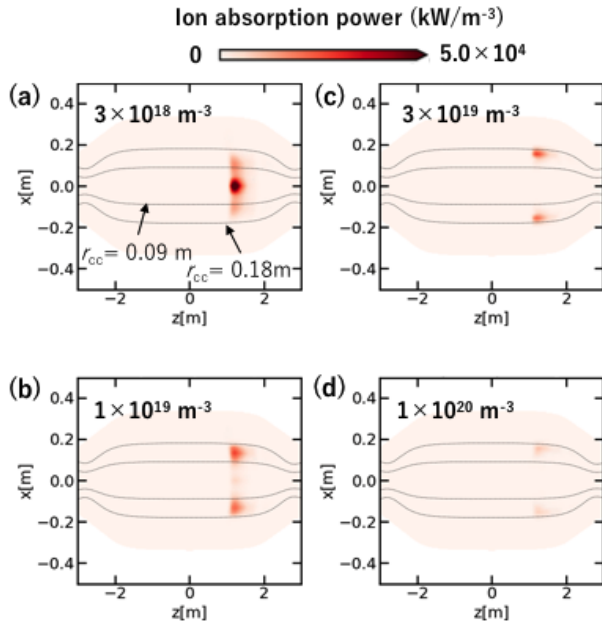


Fig. 2 Spatial distribution of ion absorption power for the density of (a) $3 \times 10^{18} \text{ m}^{-3}$, (b) $1 \times 10^{19} \text{ m}^{-3}$, (c) $3 \times 10^{19} \text{ m}^{-3}$ and (d) $1 \times 10^{20} \text{ m}^{-3}$. The dotted curves show magnetic field lines at $r_{cc} = 0.09$ and 0.18 m, where r_{cc} denotes the radius at the midplane.

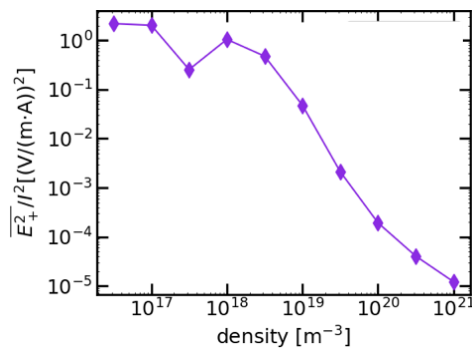


Fig. 3 Density dependence of the square of the averaged left-handed electric field strength normalized by the antenna current.

interest.

The reduction of the ion absorption power inside the plasma is caused by the variation of the field structure of the slow wave due to shielding effect. The squared intensity of the left-handed electric field that is averaged over the region including the ion cyclotron resonance layer inside the half plasma radius is shown in Fig. 3 as a function of the density. As clearly shown in Fig. 3, the squared intensity significantly decreases as the density increases; the squared intensity for the density of $1 \times 10^{20} \text{ m}^{-3}$ is less than one thousandth of that for $1 \times 10^{18} \text{ m}^{-3}$. The indentation seen at $3 \times 10^{17} \text{ m}^{-3}$ is caused by the emergence of a node near core in association with the transition of the wave structure from a fundamental eigenmode to the sec-

ond one in the radial direction.

The detail of the shielding process is shown in Fig. 4 with the variation of the spatial structure of the left-handed electric field against the increase of the density. Nine structures for the densities between $1 \times 10^{17} \text{ m}^{-3}$ and $1 \times 10^{21} \text{ m}^{-3}$ are shown in the order of the density, which is denoted by arrows. Focusing on the plasma region between the resonance around $z = 1.1$ m and the throat, it can be seen that the wave structure is a fundamental eigenmode in the radial direction and has one node in the axial direction near the resonance when the density is the lowest, $1 \times 10^{17} \text{ m}^{-3}$. For the middle in 10^{17} m^{-3} , a higher radial eigenmode emerges. For the densities in 10^{18} m^{-3} , short wavelength structures become visible near the resonance. It should be noted that the wavelength of a slow wave becomes shorter near the resonance according to the dispersion relation. In addition, the intensity near the core begins to drop in the middle of 10^{18} m^{-3} . Inside the half plasma radius, the intensity is significantly reduced when the density reaches $1 \times 10^{19} \text{ m}^{-3}$. Then, as the density further increases, the shielding region extends to the outside. As a result, a weak intensity exists at a very edge of the plasma in 10^{20} m^{-3} . For a further dense plasma, a significant shielding makes the electric field negligible except near the antenna.

4. Application of a Higher-Frequency Wave

As indicated by the simulations shown above, a shielding effect is essential when a wave is externally excited in a plasma by an RF current induced in an antenna surrounding the plasma whatever the configuration is. The frequency of a slow wave is limited by ion cyclotron frequency, then of course, an increase in a magnetic field strength reduces the shielding effect. Figure 5 (a) shows the left-handed electric field profile for $1 \times 10^{20} \text{ m}^{-3}$ density and 63.6 MHz wave frequency. Comparing with the left bottom panel in Fig. 4, the electric field strength at plasma periphery clearly recovers. The ion absorption power shown in Fig. 5 (b) shows that as the frequency increases, the absorption power increases almost linearly. About tenfold the power is available for 63.6 MHz although in that case the required field strength is quite high; 4 T and 20 T at the midplane and throat, respectively.

5. Summary

The density dependence of a slow wave excitation in the GAMMA 10/PDX central cell configuration is investigated based on a full wave calculation using TASK/WF3D code to assess the applicability of a beach heating for ion heating of a future high-density linear plasma device. The shielding effect, which a slow wave severely receives due to its low frequency, is clearly demonstrated in a three-dimensional configuration by solving Maxwell's equation as a boundary-value problem, and is well understood in the limit of cold plasma approximation. The shield-

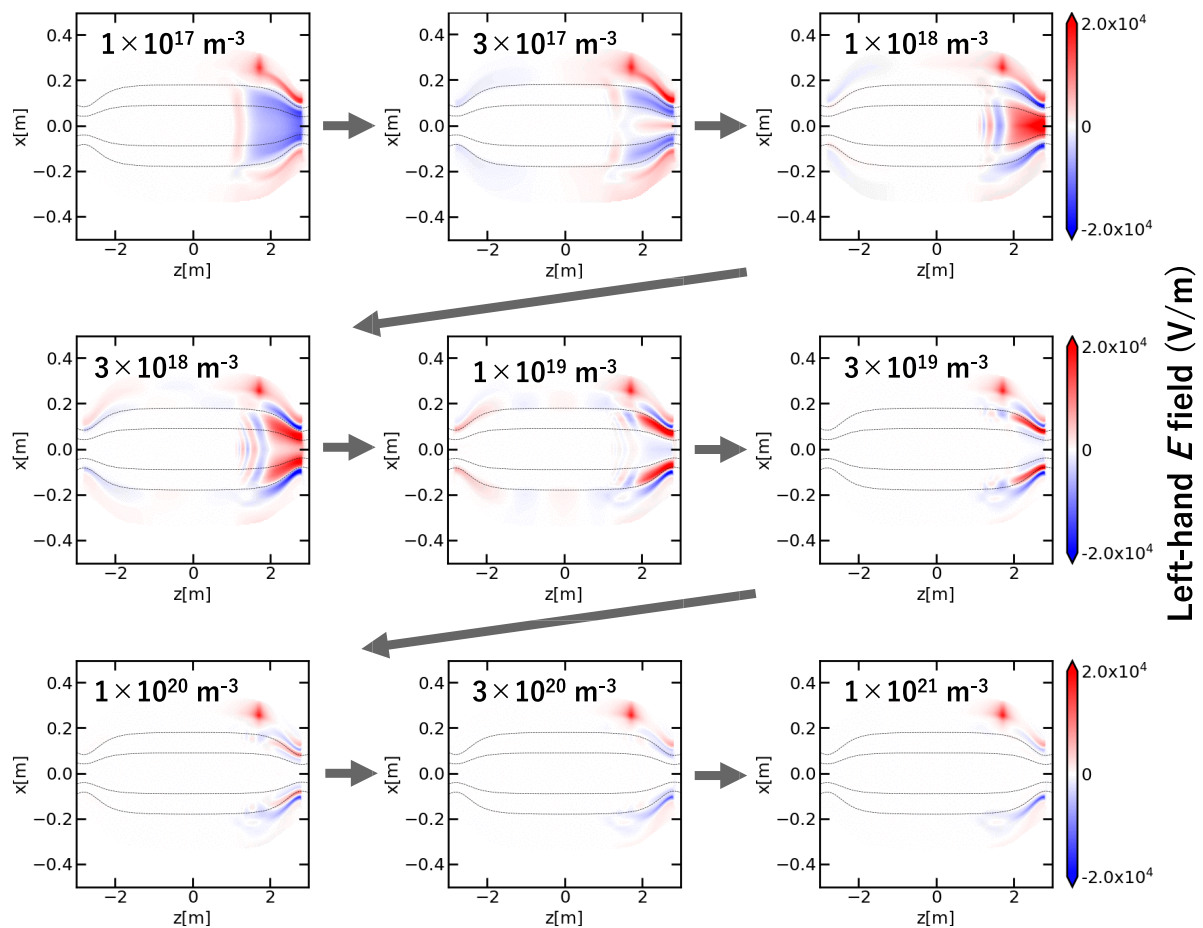


Fig. 4 Density dependence of the spatial distribution of left-handed electric field strength. All the panels have the same color scale.

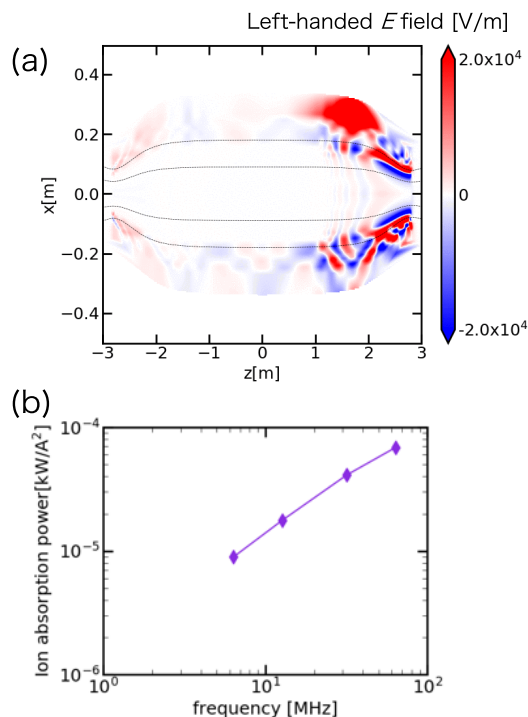


Fig. 5 (a) A left-handed electric field profile for 63.6 MHz RF current and $1 \times 10^{20} \text{ m}^{-3}$ peak density. (b) The ion absorption power dependence on the wave frequency.

ing effect becomes visible from the middle in 10^{18} m^{-3} for the 6.36 MHz wave. When the core density reaches $1 \times 10^{19} \text{ m}^{-3}$, the left-handed electric field inside the half plasma radius is significantly reduced, and thus, ion heating at only the periphery is expected. The squared electric field intensity that is averaged over the resonance region for the density of $1 \times 10^{20} \text{ m}^{-3}$ is less than one thousandth of that for $1 \times 10^{18} \text{ m}^{-3}$.

This study based on a full wave calculation indicates a difficulty in the application of a slow wave to ion heating of a high-density linear plasma. Although increases in a wave frequency, antenna current and the number of antennas help to increase a total left-handed electric field power inside a plasma, it will be still mainly localized in a low-density peripheral region. However, effect of ion heating at plasma periphery on a core plasma, namely a radial energy transport in a high-density regime, is not clarified. In addition, some favorable instabilities may appear and average the energy distribution in the radial direction, or there may be some methods to intentionally increase a radial energy transport. Furthermore, kinetic effects may change the details of the results shown in this paper. Thus, to exactly determine what extent ion heating can be expected, experimental assessments are still required. Experiments of a slow wave excitation and its measurement on a higher

density regime of GAMMA 10/PDX is being performed and will be reported in another paper.

Acknowledgments

This work was partly supported by the bidirectional collaborative research program of the National Institute for Fusion Science, Japan (NIFS14KUGM086 and NIFS17KUGM132).

- [1] Ch. Linsmeier *et al.*, Nucl. Fusion **57**, 092007 (2017).
- [2] Y. Ueda *et al.*, Nucl. Fusion **57**, 092006 (2017).
- [3] Ch. Linsmeier *et al.*, Nucl. Fusion **57**, 092012 (2017).
- [4] N. Ohno, Plasma Phys. Control. Fusion **59**, 034007 (2017).
- [5] M. Ichimura *et al.*, Nucl. Fusion **28**, 799 (1988).
- [6] M. Ichimura *et al.*, Plasma Phys. Reports **28**, 727 (2002).
- [7] J. Rapp *et al.*, Nucl. Fusion **57**, 116001 (2017).
- [8] C.J. Beers *et al.*, Phys. Plasmas **25**, 013526 (2018).
- [9] R. Ikezoe *et al.*, Fusion Sci. Technol. **68**, 63 (2015).
- [10] S. Sumida *et al.*, Fusion Sci. Technol. **68**, 136 (2015).
- [11] R. Ikezoe *et al.*, Rev. Sci. Instrum. **88**, 033504 (2017).
- [12] R. Ikezoe *et al.*, JINST **12**, C12017 (2017).
- [13] A. Fukuyama *et al.*, Proc. 20th Int. Conf. Fusion Energy, Vilamoura, Portugal, November 1–6, 2004, TH/P2-3 (2004).
- [14] Y. Yamaguchi *et al.*, Plasma Phys. Control. Fusion **48**, 1155 (2006).
- [15] T. Yokoyama *et al.*, Fusion Sci. Technol. **68**, 185 (2015).